

Multiferroic Homochiral Metal–Organic Framework

Qiong Ye,^{*,†} Da-Wei Fu,[†] Hang Tian,[†] Ren-Gen Xiong,^{*,†} Philip Wai Hong Chan,[‡] and Songping D. Huang[§]

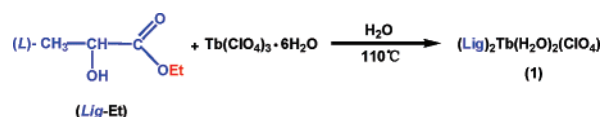
Ordered Matter Science Research Center, Southeast University, Nanjing 210096, People's Republic of China, Division of Chemistry and Biological Chemistry, School of Physical and Mathematical Sciences, Nanyang Technological University, Nanyang Avenue, Singapore 639798, Singapore, and Chemistry Department, Kent State University, Kent, Ohio 44240

Received September 16, 2007

The hydrothermal reaction of (L)-ethyl lactate (Lig-Et) with $\text{Tb}(\text{ClO}_4)_3 \cdot 6\text{H}_2\text{O}$ gives colorless block $(\text{Lig})_2\text{Tb}(\text{H}_2\text{O})_2(\text{ClO}_4)$ (**1**), in which **1** displays a laminar 2D framework. Ferroelectric and magnetic property measurements reveal that **1** probably is the first example of two “ferroic” metal–organic frameworks. Ferroelectricity of its analogue, $(\text{Lig})_2\text{Tb}(\text{D}_2\text{O})_2(\text{ClO}_4)$ (**2**), further confirms the presence of the ferroelectric deuterium effect.

Magnetism and ferroelectricity (magnetism and ferroelectricity coexist in materials called multiferroics) are essential to many forms of current technology, and the quest for multiferroic materials, where these two phenomena are intimately coupled, is of great technological and fundamental importance.^{1–3} Despite their usefulness, magnetic ferroelectrics are rare in nature, and most of them are antiferromagnets with small responses to an external magnetic field because ferroelectricity and magnetism tend to be mutually exclusive and interact weakly with each other when they coexist.⁴ However, the discovery of anomalously large interplay between ferroelectricity and magnetism in TbMnO_3 and TbMn_2O_5 has accelerated such interest.⁵ Most of the excellent multiferroic compounds are pure inorganic compounds such as BiMnO_3 and La_2MMnO_6 ($\text{M} = \text{Co}, \text{Ni}, \text{and Cu}$).⁴ Metal–organic compounds [or metal–organic framework (MOF)] have never been reported to display ferromagnetic and

Scheme 1



ferroelectric properties, to date, that we are aware of,⁶ while metal coordination compounds (or MOFs) have received widespread attention in recent years because of the ability of the organic–inorganic hybrid material to possess the useful properties of both organic (chromophore, chirality, and tailorable) and inorganic (electronic d and f orbital properties such as luminescence and magnetism) compounds within a single molecular-scale composite. In addition, metal–organic complexes offer not only increased synthetic flexibility for optimization of hyperpolarizability but also well-defined metal centers and oxidation states, which, in turn, would provide the ability to fine-tune the electronic properties of the surrounding ligands.⁷ To this end, as a continuation of systematical investigations on noncentrosymmetric compounds,⁶ we have realized that the homochiral compounds should be good candidates, with residual dipole moments leading to ferroelectric properties where the layered structures with transition-metal or rare-earth ions may mimic a perovskite structure with magnetic properties because transition-metal ions have unpaired electrons to result in the occurrence of magnetism while a homochiral ligand ensures the MOF to crystallize in an acentric space group. The hydrothermal reaction of $\text{Tb}(\text{ClO}_4)_3 \cdot 6\text{H}_2\text{O}$ with (L)-ethyl lactate (Lig-Et) offers one 2D laminar homochiral MOF, $(\text{Lig})_2\text{Tb}(\text{H}_2\text{O})_2(\text{ClO}_4)$ (**1**), as shown in Scheme 1.

* To whom correspondence should be addressed. E-mail: yeqiong@seu.edu.cn (Q.Y.), xiongrg@seu.edu.cn (R.-G.X.).

[†] Southeast University.

[‡] Nanyang Technological University.

[§] Kent State University.

- (1) (a) Bune, A. V.; Fridkin, V. M.; Ducharme, S.; Blinov, L. M.; Palto, S. P.; Sorokin, A. V.; Yudin, S. G.; Zlatkin, A. *Nature* **1998**, *391*, 874. (b) Fiebig, M.; Lottermoser, Th.; Frohlich, D.; Goltsev, A. V.; Pisarev, R. V. *Nature* **2002**, *424*, 818.
- (2) Eerenstein, W.; Mathur, N. D.; Scott, J. F. *Nature* **2006**, *442*, 759.
- (3) Cheong, S. W.; Mostovoy, M. *Nature Mater.* **2007**, *6*, 13.
- (4) Azuma, M.; Takata, K.; Saito, T.; Ishiwata, S.; Shimakawa, Y.; Takano, M. *J. Am. Chem. Soc.* **2005**, *127*, 8889.
- (5) (a) Kimura, T.; Goto, T.; Shintani, H.; Ishizaka, K.; Arima, T.; Tokura, Y. *Nature* **2003**, *426*, 55. (b) Hur, N.; Park, S.; Sharma, P. A.; Ahn, J. S.; Guha, S.; Cheong, S.-W. *Nature* **2004**, *429*, 392.

- (6) For ferroelectric MOFs, see: (a) Qu, Z.-R.; Zhao, H.; Wang, Y.-P.; Wang, X.-S.; Ye, Q.; Li, Y.-H.; Xiong, R.-G.; Abrahams, B. F.; Liu, Z.-G.; Xue, Z.; You, X.-Z. *Chem.—Eur. J.* **2004**, *10*, 53. (b) Okubo, T.; Kawajiri, R.; Mitani, T.; Shimoda, T. *J. Am. Chem. Soc.* **2005**, *127*, 17598. (c) Zhao, H.; Qu, Z.-R.; Ye, Q.; Abrahams, B. F.; Wang, Y.-P.; Liu, Z.-G.; Xue, Z.; Xiong, R.-G. *Chem. Mater.* **2003**, *15*, 4166. (d) Ye, Q.; Song, Y.-M.; Wang, G.-X.; Chen, K.; Fu, D.-W.; Chan, P. W. H.; Zhu, J.-S.; Huang, S. D.; Xiong, R.-G. *J. Am. Chem. Soc.* **2006**, *128*, 6554. (e) Zhao, H.; Qu, Z.-R.; Ye, H.-Y.; Xiong, R.-G. *Chem. Soc. Rev.* **2008**, *37*, 84.
- (7) Mitzi, D. B.; Chondroudis, K.; Kagan, C. R. *IBM J. Res. Dev.* **2001**, *45*, 29.

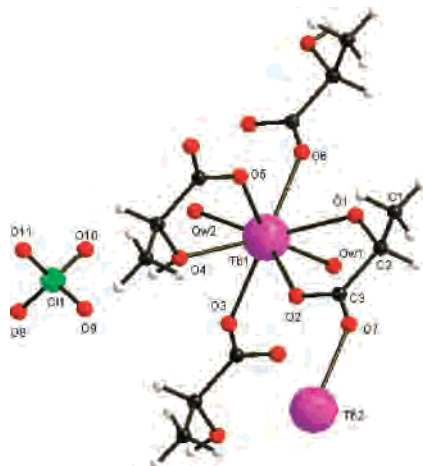


Figure 1. Asymmetric unit of 2D MOF **1** in which the local coordination environment around the Tb ion has a slightly distorted square antiprism while the perchlorate ion fails to take part in the coordination to the Tb ion and serves only as a charge balance ion. The color codes green, red, purple, black, and white balls indicate Cl, O, Tb, C, and H atoms, respectively. Typical bond distances (Å): Tb1–O3 2.291(19), Tb1–O2 2.320(17), Tb1–O4 2.325(15), Tb1–O1 2.416(14), Cl1–O6 1.30(3), Cl1–O5 1.39(4).

The IR spectrum of MOF **1** shows that there is a very strong peak at 1105 cm^{-1} , probably indicating the presence of a perchlorate ion, while three strong peaks at 1604, 1470, and 1434 cm^{-1} are suggestive of a carboxylate ion. As expected, a broad peak at 3480 cm^{-1} probably suggests the presence of water in MOF **1**.⁸

X-ray crystal structure determination of MOF **1** shows that the local coordination environment around the Tb ion can be best described as a slightly distorted square antiprism or dodecahedron, where six O atoms come from four different lactate ions while two water molecules completed the eight-coordination mode (Figure 1).⁹ Thus, each lactate ion links two Tb ions using one of the two O atoms of carboxylate and hydroxy groups to chelate the Tb ion while the other O atom of carboxylate bridges another Tb ion to result in the formation of a 2D-layered framework, as depicted in Figure 2. A careful investigation of Figure 2 reveals that a cation

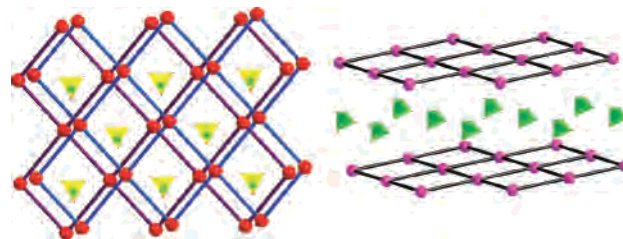


Figure 2. Two simplified 2D laminar network representations in which the cation 2D square $\text{Tb}(\text{lactate})_2$ acts as the sides of the sandwich to intercalate perchlorate ions along two different crystallographic directions (the ball stands for the Tb ion, while straight line is the lactate ligand).

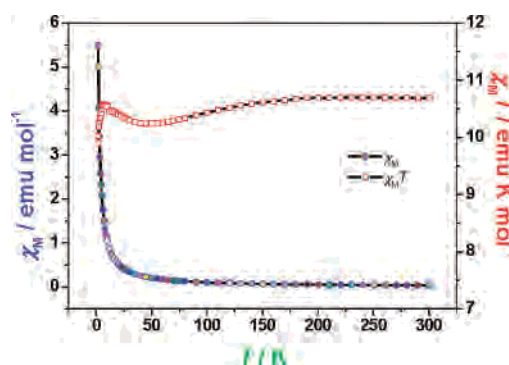


Figure 3. Temperature dependence of magnetic susceptibilities in the form of $\chi_m T$ and χ_m at an applied field of 2 kOe from 1.8 to 300 K for MOF **1**.

laminar layer $\text{Tb}(\text{Lig})_2$, used as the sides of a sandwich to intercalate perchlorate ions, results in the formation of a 3D framework through hydrogen bonds (see the Supporting Information).

Figure 3 shows the temperature dependence of the magnetic susceptibility in the form of $\chi_m T$ vs T for MOF **1**. The magnetic property from the $\chi_m T$ vs T curve seems too complicated to fit by any equation. As seen in Figure 3, the $\chi_m T$ curve of MOF **1** slowly decreases from ca. $10.7\text{ emu}\cdot\text{K}\cdot\text{mol}^{-1}$ at 300 K to a minimum of $10.5\text{ emu}\cdot\text{K}\cdot\text{mol}^{-1}$ at 41 K with temperature cooling and then gradually increases, basically returning to a value of $10.636\text{ emu}\cdot\text{K}\cdot\text{mol}^{-1}$ at 6 K, and subsequently goes down sharply to $9.8\text{ emu}\cdot\text{K}\cdot\text{mol}^{-1}$ at 1.8 K. Such magnetic behavior has been recently reported for dinuclear $[\text{ErL}_3(\text{H}_2\text{O})_2]_2\cdot 4\text{H}_2\text{O}$ ($\text{L} = \text{salicylic acid}$) and $[\text{Er}_2(\text{L})(\text{HL})(\text{NO}_3)_6(\text{HCOO})]\cdot 3\text{MeOH}$ [$\text{L} = 1,3,5\text{-tris}(\text{imidazol-1-ylmethyl})\text{-2,4,6-trimethylbenzene}$].¹⁰ The temperature dependence of magnetic behavior also seemingly indicates ferromagnetic coupling between the Tb^{III} ions in MOF **1**.

Given that product **1** crystallizes in a chiral space group (C_2) while it also adopts a polar space group, its optical properties were investigated. Preliminary studies of the powdered sample indicate that **1** is second-harmonic-generation-active, with approximately 1 times that of KDP.¹¹ The space group C_2 is associated with the point group C_2 , one of the 10 polar point groups required for ferroelectric behavior. Experimental results indicate that MOF **1** does indeed display ferroelectric behavior. Figure 4 clearly shows

(8) **Synthesis of 1:** The hydrothermal reaction of (L)-ethyl lactate (1.0 mL) in the presence of $\text{Tb}(\text{ClO}_4)_3\cdot 6\text{H}_2\text{O}$ (1 mmol) with 1.5 mL of water in a sealed Pyrex tube at $110\text{ }^\circ\text{C}$ for 2–4 days gave colorless block compound **1** in 50% yield based on $\text{Tb}(\text{ClO}_4)_3\cdot 6\text{H}_2\text{O}$ after cooling down. IR (cm^{-1}): 3480 (s, br), 2980 (vw), 2937 (vw), 1603 (vs), 1470 (m), 1434 (m), 1359 (m), 1315 (w), 1241 (w), 1105 (vs), 933 (w), 870 (w), 781 (w), 628 (w), 570 (w), 452 (w). Anal. Calcd for $\text{C}_6\text{H}_{14}\text{ClO}_{12}\text{Tb}$: C, 15.24; H, 2.96. Found: C, 15.30; H, 3.01. TGA suggests that MOF **1** can be stable before ca. $200\text{ }^\circ\text{C}$ (see the Supporting Information). **Synthesis of 2:** The hydrothermal reaction of (L)-ethyl lactate (1.0 mL) in the presence of $\text{Tb}(\text{ClO}_4)_3\cdot 6\text{H}_2\text{O}$ (1 mmol) with 1.5 mL of deuterated oxide (D_2O) in a sealed Pyrex tube at $110\text{ }^\circ\text{C}$ for 2–4 days gave colorless block compound **2** in 45% yield based on $\text{Tb}(\text{ClO}_4)_3\cdot 6\text{H}_2\text{O}$ after cooling down. IR (cm^{-1}): 3466 (s, br), 2980 (vw), 2937 (vw), 2515 (m), 1602 (vs), 1465 (m), 1433 (m), 1358 (m), 1313 (w), 12413 (w), 1107 (vs), 934 (w), 868 (w), 777 (w), 628 (w), 567 (w), 451 (w). Anal. Calcd for $\text{C}_6\text{H}_{10}\text{D}_4\text{ClO}_{12}\text{Tb}$: C, 15.11; H, 2.10. Found: C, 15.18; H, 2.07.

(9) Crystal data of **1**: $\text{C}_6\text{H}_{14}\text{ClO}_{12}\text{Tb}$, $M = 472.54$, monoclinic, C_2 , $a = 8.635(2)\text{ \AA}$, $b = 8.3357(19)\text{ \AA}$, $c = 10.187(2)\text{ \AA}$, $\beta = 92.002(4)^\circ$, $V = 732.8(3)\text{ \AA}^3$, $Z = 2$, $D_c = 2.142\text{ Mg}\cdot\text{m}^{-3}$, $R_1 = 0.0473$, $wR_2 = 0.1341$, $\mu = 5.062\text{ mm}^{-1}$, $S = 1.092$; Flack parameter = 0.08(4). Crystal data of **2**: $\text{C}_6\text{H}_{10}\text{D}_4\text{ClO}_{12}\text{Tb}$, $M = 476.57$, monoclinic, C_2 , $a = 8.6580(15)\text{ \AA}$, $b = 8.3628(18)\text{ \AA}$, $c = 10.2187(18)\text{ \AA}$, $\beta = 91.933(2)^\circ$, $V = 739.5(2)\text{ \AA}^3$, $Z = 2$, $D_c = 2.140\text{ Mg}\cdot\text{m}^{-3}$, $R_1 = 0.0460$, $wR_2 = 0.1009$, $\mu = 5.016\text{ mm}^{-1}$, $S = 1.055$; Flack parameter = 0.01(4).

(10) (a) Costes, J.-P.; Clemente-Juan, J. M.; Dahan, F.; Nicodème, F.; Verelst, M. *Angew. Chem., Int. Ed.* **2002**, *41*, 323. (b) Zhang, Z.-H.; Song, Y.; Okamura, T.; Hasegawa, Y.; Sun, W.-Y.; Ueyama, N. *Inorg. Chem.* **2006**, *45*, 2896.

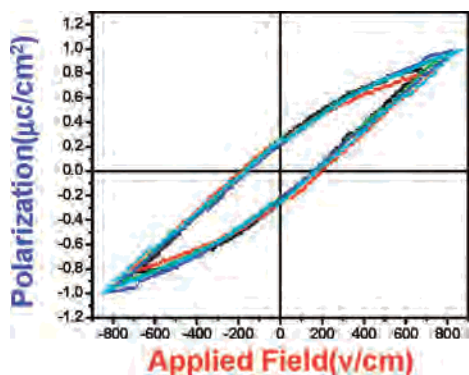


Figure 4. Electric hysteresis loop of a pellet of powders of MOF 1 observed by an RT6000 ferroelectric tester at room temperature (the different curves stand for different hysteresis loops at different voltage measurements).

that there is an electric hysteresis loop, which is a typical ferroelectric feature, with a remanent polarization (P_r) of ca. $0.25 \mu\text{C}\cdot\text{cm}^{-2}$ and a coercive field (E_c) of $0.2 \text{ kV}\cdot\text{cm}^{-1}$. The saturation spontaneous polarization (P_s) of **1** is ca. $1.0 \mu\text{C}\cdot\text{cm}^{-2}$, which is smaller than those of the typical ferroelectrics KDP ($P_s = 5.0 \mu\text{C}\cdot\text{cm}^{-2}$) and triglycine sulfate (TGS; $P_s = 3.0 \mu\text{C}\cdot\text{cm}^{-2}$) but larger than that of $\text{NaKC}_4\text{H}_4\text{O}_6\cdot 4\text{H}_2\text{O}$ (Rosal salt; $P_s = 0.25 \mu\text{C}\cdot\text{cm}^{-2}$). To further confirm the ferroelectric behavior of MOF **1**, we have performed the synthesis and crystal structure determination of $(\text{Lig})_2\text{Tb}(\text{D}_2\text{O})_2(\text{ClO}_4)$ (**2**), in which a medium peak at 2515 cm^{-1} suggests the presence of D_2O while other typical peaks of ClO_4^- and carboxylate groups are basically identical with those of MOF **1** (see the Supporting Information). Crystal structural determination reveals that MOF **2** is isostructural to that of MOF **1**. Figure 2S in the Supporting Information also clearly shows that there is an electric hysteresis loop, which is a typical ferroelectric feature, with a remanent polarization (P_r) of ca. $0.90 \mu\text{C}\cdot\text{cm}^{-2}$ and a coercive field (E_c) of $0.33 \text{ kV}\cdot\text{cm}^{-1}$. The saturation spontaneous polarization (P_s) of **2** is ca. $2.03 \mu\text{C}\cdot\text{cm}^{-2}$. Thus, the deuteration effect of P_r and P_s should be 3.6 and 2.03 times that of nondeuterated MOF **1**, respectively. On the other hand, the smaller coercive field is comparable to those found in the organic compounds and polymers.¹² Thus, to the best of our knowledge, **1** represents the first example of MOFs that exhibit ferromagnetic and ferroelectric properties that coexist.

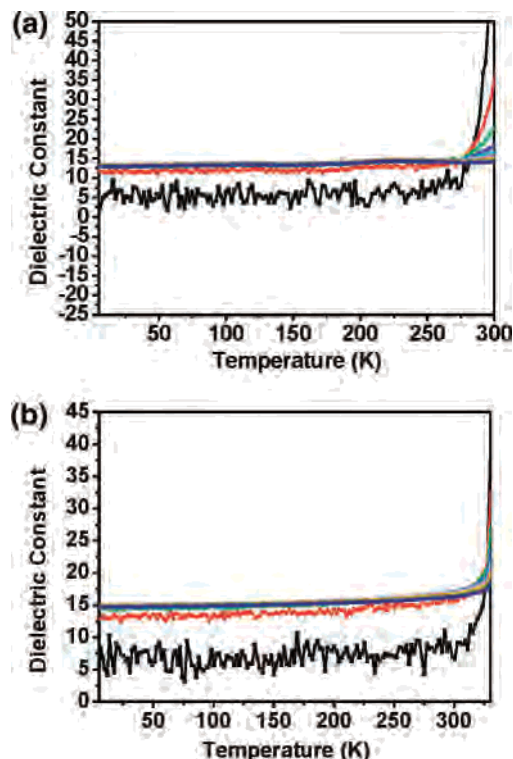


Figure 5. (a) Dielectric permittivity (ϵ_r) of powdered sample **1** as a function of the temperature. The measurements were only taken at a high frequency of 1 MHz because there is no fluctuation during measurement (the different curves stand for the different dielectric constants measured at different frequencies from 10^2 , $10^{2.5}$, 10^3 , $10^{3.5}$, 10^4 , $10^{4.5}$, 10^5 , $10^{5.5}$ to 10^6 Hz starting from the bottom).¹³ (b) Dielectric permittivity (ϵ_r) of powdered sample **2** as a function of the temperature. The measurements were only taken at a high frequency of 1 MHz because there is no fluctuation during measurement (the different curves stand for the different dielectric constants measured at different frequencies from 10^2 , $10^{2.5}$, 10^3 , $10^{3.5}$, 10^4 , $10^{4.5}$, 10^5 , $10^{5.5}$ to 10^6 Hz starting from the bottom).¹³

On the other hand, their ferroelectric properties should be associated with relatively high dielectric constants. To verify that both MOFs **1** and **2** possess high dielectric constants, the powdered samples were measured at different frequencies and temperatures, as shown in Figure 5. From Figure 5a,b, it can be seen that MOFs **1** and **2** both display relatively high dielectric constants, reaching at ca. 13 and 15, respectively. In addition, we can estimate the deuteration effect on permittivity, being about 15% [$= (15 - 13)/13$].

In summary, a 2D laminar multiferroic MOF was prepared through employment of esterification under hydrothermal reaction conditions. This class of materials provides a new impetus to examining the potential applications of MOFs as multiferroic materials.

Acknowledgment. This work was supported by the 973 project (Grant G2000077500), National Natural Science Foundation of China, and EYTP of MOE, People's Republic of China. R.-G.X. thanks Dr. Y. Song for magnetic measurements and the reviewers for their excellent suggestions.

Supporting Information Available: Detailed experimental procedures, IR spectroscopic data, additional ORTEP views, and X-ray crystallographic CIF files. This material is available free of charge via the Internet at <http://pubs.acs.org>.

IC701828W

- (11) (a) Ye, Q.; Wang, X.-S.; Zhao, H.; Xiong, R.-G. *Chem. Soc. Rev.* **2005**, *34*, 208. (b) Xiong, R.-G.; Xue, X.; Zhao, H.; You, X.-Z.; Abrahams, B. F.; Xue, Z. L. *Angew. Chem., Int. Ed.* **2002**, *41*, 3800. (c) Tang, Y.-Z.; Huang, X.-F.; Song, Y.-M.; Chan, P. W. H.; Xiong, R.-G. *Inorg. Chem.* **2006**, *45*, 4868. (d) Ye, Q.; Li, Y.-H.; Song, Y.-M.; Huang, X.-F.; Xiong, R.-G.; Xue, Z. L. *Inorg. Chem.* **2005**, *44*, 3618. (e) Wang, X.-S.; Tang, Y.-Z.; Huang, X.-F.; Qu, Z.-R.; Che, C.-M.; Chan, P. W. H.; Xiong, R.-G. *Inorg. Chem.* **2005**, *44*, 5278. (f) Ye, Q.; Tang, Y.-Z.; Wang, X.-S.; Xiong, R.-G. *Dalton Trans.* **2005**, 1570. (g) Qu, Z.-R.; Zhao, H.; Wang, X.-S.; Li, Y.-H.; Song, Y.-M.; Liu, Y.-J.; Ye, Q.; Xiong, R.-G.; Abrahams, B. F.; Xue, Z. L.; You, X.-Z. *Inorg. Chem.* **2003**, *43*, 7710.
- (12) (a) Horiuchi, S.; Kumai, R.; Tokura, Y. *J. Am. Chem. Soc.* **2005**, *127*, 5010. (b) Furukawa, T. *Phase Transitions* **1989**, *18*, 143.
- (13) (a) Fu, D.-W.; Song, Y.-M.; Wang, G.-X.; Ye, Q.; Xiong, R.-G.; Akutagawa, T.; Nakamura, T.; Chan, P. W. H.; Huang, S. D. *J. Am. Chem. Soc.* **2007**, *129*, 5346. (b) Ye, Q.; Zhao, H.; Qu, Z.-R.; Fu, D.-W.; Xiong, R.-G.; Cui, Y.-P.; Akutagawa, T.; Chan, P. W. H.; Nakamura, T. *Angew. Chem., Int. Ed.* **2007**, *46*, 6852. (c) Zhao, H.; Ye, Q.; Qu, Z.-R.; Fu, D.-W.; Xiong, R.-G.; Huang, S. D.; Chan, P. W. H. *Chem.—Eur. J.* **2007**, website available.